Journal of Materials Science and Chemical Engineering, 2024, 12, 61-72
https://www.scirp.org/journal/msce
ISSN Online: 2327-6053
ISSN Print: 2327-6045

# Study on Acoustic Emission Characteristics of Deformation Damage Process of Zirconia Ceramics

**Qingchuan Fu[1], Yushu Lai[2*]**

[1]School of Electronic Information and Engineering, Chongqing Three Gorges University, Chongqing, China
[2]Key Laboratory of Signal and Information Processing, School of Electronic and Information Engineering, Chongqing Three Gorges University, Chongqing, China
Email: *laser121@sina.com

**How to cite this paper:** Fu, Q.C. and Lai, Y.S. (2024) Study on Acoustic Emission Characteristics of Deformation Damage Process of Zirconia Ceramics. *Journal of Materials Science and Chemical Engineering*, **12**, 61-72.
https://doi.org/10.4236/msce.2024.122005

**Received:** January 26, 2024
**Accepted:** February 24, 2024
**Published:** February 27, 2024



## Abstract

Zirconia ceramics have become increasingly widely used in recent years and are favored by relevant enterprises. From the traditional dental field to aerospace, parts manufacturing has been used, but there is limited research on the deformation and damage process of zirconia ceramics. This article analyzes the acoustic emission characteristics of each stage of ceramic damage from the perspective of acoustic emission, and explores its deformation process characteristics from multiple perspectives such as time domain, frequency, and EWT modal analysis. It is concluded that zirconia ceramics exhibit higher brittleness and acoustic emission strength than alumina ceramics, and when approaching the fracture, it tends to generate lower frequency acoustic emission signals.

## Keywords

Zirconia Ceramics, Acoustic Emission Monitoring, Crack Damage

## 1. Introduction

In recent years, zirconia ceramic materials have been applied from traditional dentistry to aerospace, parts manufacturing, artificial bones and other fields due to their advantages of high melting point, wear resistance, corrosion resistance, and good biocompatibility [1] [2] [3] [4] [5]. At present, scholars have a strong interest in various physical and chemical studies of zirconia, and most of the research on this material focuses on its processing and structural characteristics

[6] [7] [8] [9] [10]. There is relatively little research on the characteristics exhibited during crack damage and deformation. The research on ceramic materials has a history of several decades, but scholars still have great interest in the study of high-performance ceramic properties [11] [12] [13] [14] [15]. Ceramic products are widely used, and when ceramic materials undergo deformation and damage, such internal damage and crack propagation are difficult to observe. When studying the performance of materials, acoustic emission technology is widely used in the field of material monitoring because it relies on the signals emitted by the tested object itself to make relevant judgments and analysis, which will not cause secondary damage to the material. At the same time, it meets the requirements of monitoring the state in complex and invisible environments [16] [17]. Guo Li [18] studied the wear status of diamond grinding wheels during zirconia ceramic machining and grinding using EMD decomposition and acoustic emission technology in monitoring the wear status of diamond grinding wheels. Sebasti á n E. Gass *et al.* [19] studied the mechanical properties of ceramic materials at high temperatures. Anders Sundh *et al.* [20] studied the application and flexural strength of zirconia ceramic products in dentistry. D. Giridhar *et al.* [21] studied the acoustic emission characteristics of alumina zirconia composite ceramics during processing, and obtained the differences in acoustic emission characteristics under different processing modes. Chu Liang and Chang Zhisheng [22] [23] conducted acoustic emission signal monitoring on the Brazilian splitting test process of zirconia toughened alu-mina, and found that zirconia toughened alumina ceramics have higher fracture tough-ness compared to alumina ceramics without toughening effect. Scholars have also con-ducted relevant studies on the fracture toughness of zirconia ceramics under different conditions [24] [25] [26] [27]. When studying the deformation and damage of zirconia ceramics, many cracks are excited. There are many ways to study material cracks, including the ratio of rise ratio to peak amplitude, ringing count, signal analysis, etc. [28] [29]. This article conducts acoustic emission monitoring on the stress damage process of 99 type alumina and 95 type zirconia, in order to obtain the crack evolution law and acoustic emission characteristics of different damage stages of the two materials.

## 2. Experimental Materials and Plans

The materials used in this experiment are all from Suzhou Qianen Special Ceramics Company in China. The new type of zirconia ceramics has many unknown characteristics compared to traditional alumina ceramics. In the experiment, the acoustic emission characteristics of 99 type alumina ceramics and 95 type zirconia ceramics, which are commonly seen in the market, were compared when subjected to deformation damage under external forces. This can provide a mechanism for material fracture, prevent possible ad-verse effects, or provide valuable reference for material process progress. Among them, Type 99 alumina is a high-purity alumina ceramic, while Type 95 zirconia ceramic is a yttrium

stable type with a yttrium oxide content of about 5%. The experimental system diagram is shown in Figure 1. The experimental materials are 95 zirconia ceramic and 99 alumina ceramic, with five parts each, and the specifications are 60 * 10 * 5 mm for both materials.

The percolation theory of acoustic emission suggests that the crack damage of ceramics is caused by the continuous propagation of internal cracks under external stress [30] [31]. By applying a constant speed external force to the experimental specimen, the crack damage of ceramic specimens under external force is simulated, and the acoustic emission signals of each stage are monitored through the acoustic emission system. The loading speed used in the experiment is all 0.1 mm/min, with a span of 60 mm. The experimental plan is to apply mechanical stress downwards at a constant speed until the ceramic plate fractures.

## 3. Experimental Results and Signal Analysis

### 3.1. Material Counting Rate Analysis

Acoustic emission count refers to the number of times an instrument collects waveforms that exceed the set threshold per unit time. Generally speaking, the higher the ring count, the more frequent the acoustic emission activity. It has important reference significance in studying material damage and crack propagation. For the convenience of observing 95 zirconia in units of 10 seconds and 99 alumina in units of 5 seconds, count their ringing times. From Figure 1, it can be seen that the fracture process of 95 zirconia ceramics collected more ringing counts, indicating that its material strength is much higher than that of 99 type alumina, as the former requires higher fracture energy for fracture. The acoustic emission process of these two materials can be divided into the following stages based on the variation of ringing count over time. Firstly, there is 95 type zirconia ceramic, with 0 - 50 s as the initial compaction stage, 50 - 450 s as

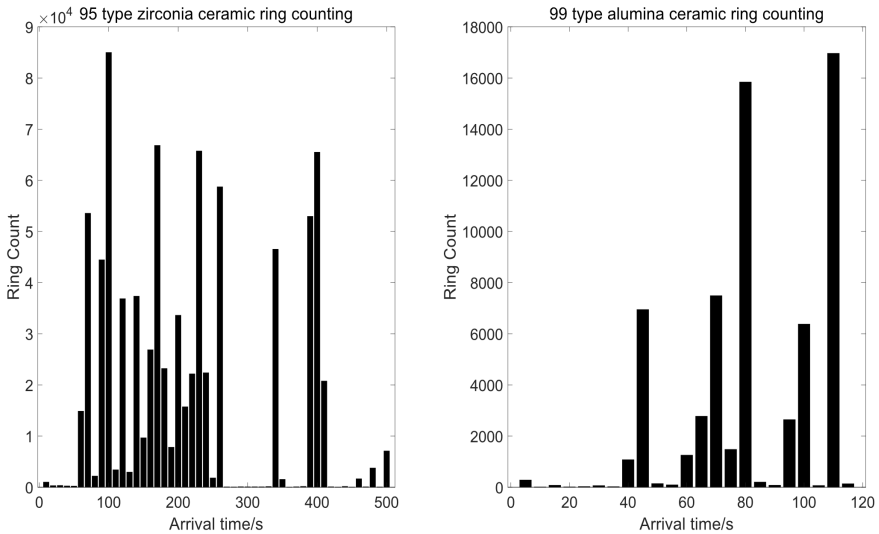


Figure 1. Ring counting analysis of two types of ceramics.

the crack propagation stage, and 450 - 496 s as the critical instability stage. Next is the 99 type alumina ceramic, which is in the initial compaction stage from 0 to 30 seconds, the crack propagation stage from 30 to 100 seconds, and the critical instability stage from 100 to 110 second.

### 3.2. Signal and Energy Analysis of Materials

**Figure 2** and **Figure 3** represent the time-frequency domain of 95 type zirconia and 99 type alumina, respectively. The upper half of each figure is a time-domain graph, and the lower half is the corresponding frequency-domain graph. It can be observed that the amplitude in the time domain is relatively low during the initial compaction stage, and the proportion of high-frequency components is higher than the other two stages. The signal amplitude collected at the critical instability point is the highest, while the low-frequency component content increases. In the later stage of fracture, it can be clearly detected that the low-frequency signal components reach high values, and the amplitude of the signal in the time domain is also high. The critical instability point is the time close to fracture, and the later stage of fracture refers to the end of the fracture process. The interval between their experiments usually does not exceed 2 seconds. It can be considered that there is a risk of fracture in ceramic materials when a large number of low-frequency component acoustic emission signals are detected. 95 type zirconia ceramics emit more and stronger signals when subjected to force fracture than 99 type zirconia ceramics.

Now, analyzing the acoustic emission signals collected from the critical instability points in **Figure 2** and **Figure 3**, the EMD (Empirical Mode Decomposition) method is considered suitable for handling nonlinear and non-stationary signals, but it has drawbacks such as mode aliasing and high computational complexity. EWT [32] (Empirical Mode Decomposition) solves the problem of mode aliasing caused by improper convergence conditions in EMD decomposition, with smaller computational complexity and fewer modes. However, the various modes obtained from EWT decomposition need to be screened and evaluated. The traditional method is to directly select based on the spectrum, which is suitable for researchers who know their own research frequency band, and the screening effect on unknown frequency bands is not good. In response to this, the method used in this experiment is EWT + kurtosis + correlation analysis. EWT related formulas 1 and 2 are shown.

$$\psi_n(\omega)=\begin{cases}1, & \omega_n+\tau_n\le|\omega|\le\omega_{n+1}-\tau_{n+1}\\ \cos\left[\frac{\pi}{2}\beta\left(\frac{1}{2\tau_{n+1}}\left(|\omega|-\omega_{n+1}+\tau_{n+1}\right)\right)\right], & \omega_{n+1}-\tau_{n+1}\le|\omega|\le\omega_{n+1}+\tau_{n+1}\\ \sin\left[\frac{\pi}{2}\beta\left(\frac{1}{2\tau_n}\left(|\omega|-\omega_n+\tau_n\right)\right)\right], & \omega_n-\tau_n\le|\omega|\le\omega_n+\tau_n\\ 0, & \text{others}\end{cases} \tag{1}$$

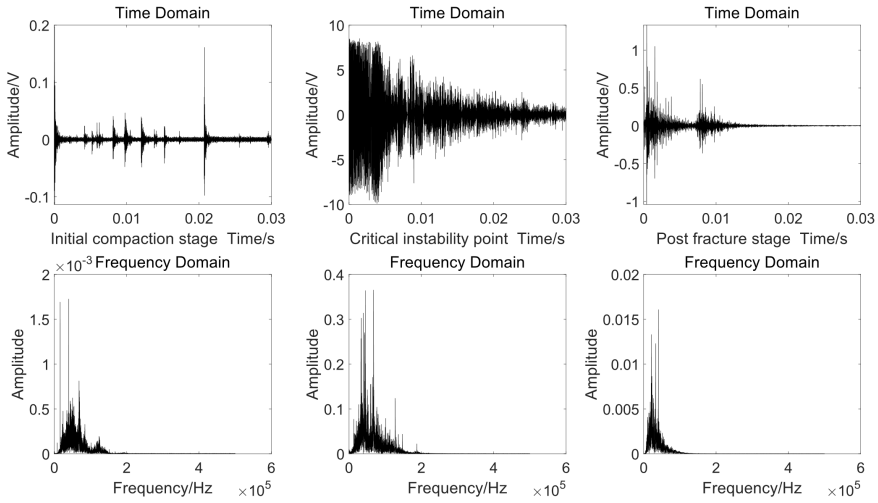


**Figure 2.** Signal diagram of type 95 zirconia ceramic.

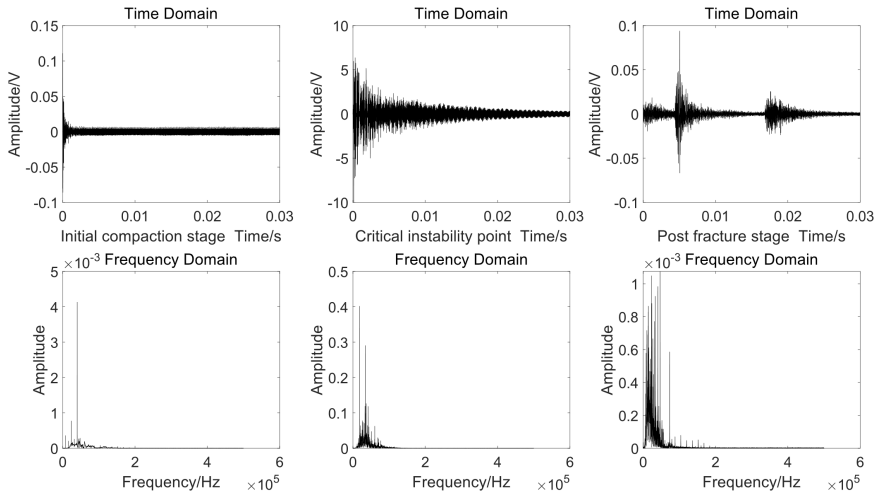


**Figure 3.** Signal diagram of Type 99 alumina ceramic.

$$\varphi_n(\omega)=\begin{cases}1, & |\omega|\le\omega_n-\tau_n\\ \cos\left[\dfrac{\pi}{2}\beta\left(\dfrac{1}{2\tau_n}\left(|\omega|-\omega_n+\tau_n\right)\right)\right], & \omega_n-\tau_n\le|\omega|\le\omega_n+\tau_n\\ 0, & \text{others}\end{cases} \quad (2)$$

where in $\beta(x)=x^4\left(35-84x+70x^2-20x^3\right)$, n > 0, $\varphi_n(\omega)$ represents the empirical wavelet function, $\varphi_n(\omega)$ represents the empirical scale function, $\omega_n$ represents the center frequency of each frequency band, $\tau_n$ represents the boundary bandwidth.

The critical point signal analysis of 95 zirconia is shown in **Figure 4**. It can be seen that EMD decomposes into 8 IMF components and 1 res component. The correlation coefficients of IMF1-IMF8 are 0.931, 0.301, 0.018, 0.005, 0.003, 0.004, 0.003, −0.002, and 0.001, respectively. At the same time, the kurtosis of IMF1-IMF8 are 8.007, 8.570, 8.396, 11.073, 5.175, 7.341, 4.425, 2.297, and the

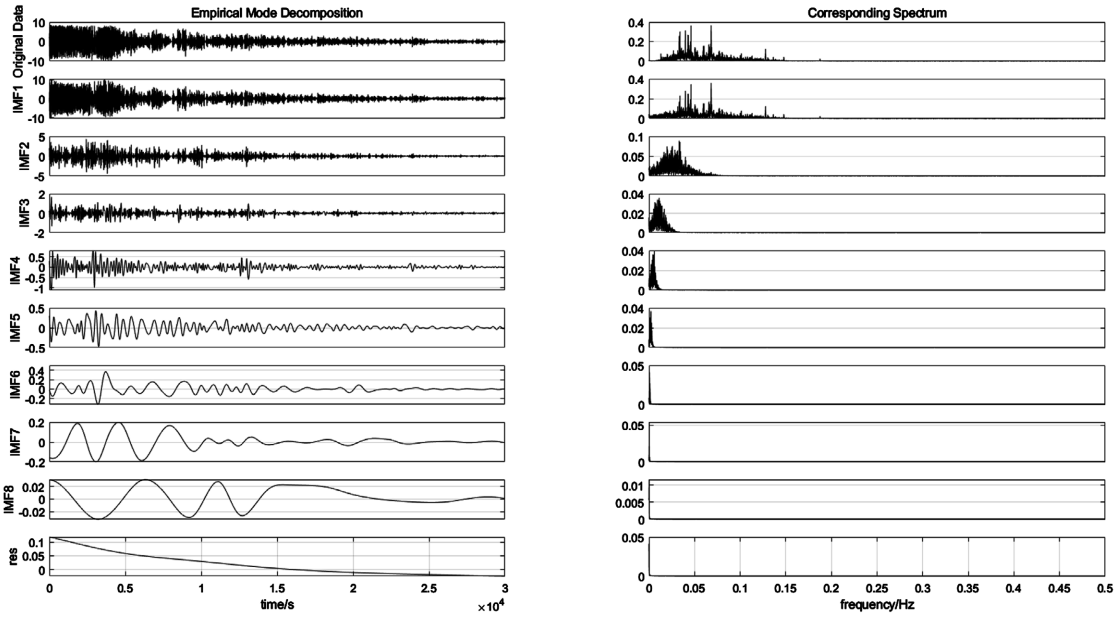


**Figure 4.** Empirical mode decomposition of critical instability point for 95 type zirconia ceramics.

kurtosis of the res component is 2.771. The EWT de-composition of the signal is shown in Figure 5, and it can be observed that the modes are significantly reduced, with a total of one mra component and one res component. The correlation coefficient of mra1 is 0.776, with a kurtosis of 12.636, and the correlation coefficient of res is 0.770, with a kurtosis of 7.378. The range of correlation coefficient values is [−1, 1], and the closer the correlation coefficient is to 1, the more similar the two signals are. Kurtosis represents the distribution of signal extremes, and generally, larger values contain more noise. From the above, it can be seen that EMD decomposes into many invalid modes, which are difficult to analyze. But EWT decomposed fewer modes, relatively easier to analyze. According to the kurtosis and correlation criteria, the res mode decomposed by EWT is more representative of the signal, indicating that the critical point signal has more relative low-frequency components.

Figure 6 shows the analysis of the critical point signal of 99 alumina, which is still divided into two modes. The correlation coefficient of mra1 is 0.093, with a kurtosis of 73.377, and the correlation coefficient of res is 0.999, with a kurtosis of 18.744. By relying on the above evaluation criteria, the res mode can better represent the characteristics of the original signal, and it can also be concluded that the critical point signal has more low-frequency components.

Table 1 and Table 2 respectively summarize the energy and amplitude characteristics of each stage. It can be seen that the 95 type zirconia ceramic releases less acoustic emission energy in the initial stage of the bending experiment, and its acoustic emission energy is mainly generated during the crack propagation stage. The highest amplitude of the acoustic emission signal was detected during the final instability stage, but the number of acoustic emission energies exceeding 200 mV * us was not very high. However, during the initial compaction

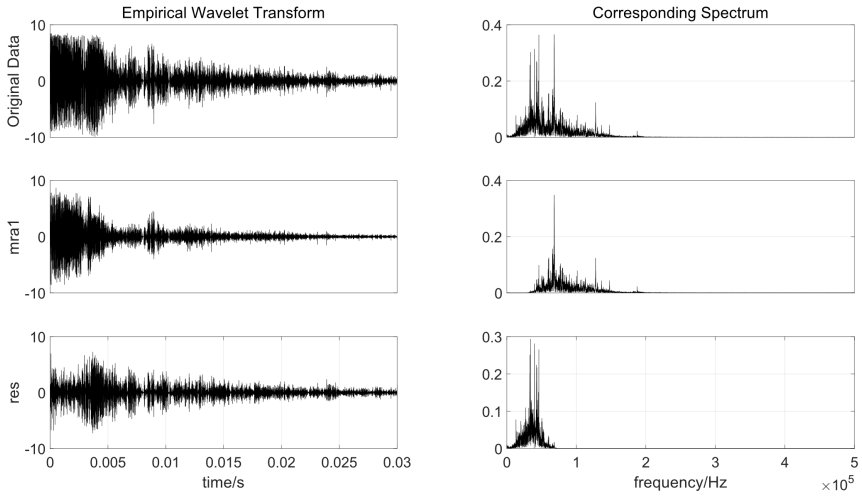


**Figure 5.** Empirical wavelet transform of critical instability point for 95 type zirconia ceramics.

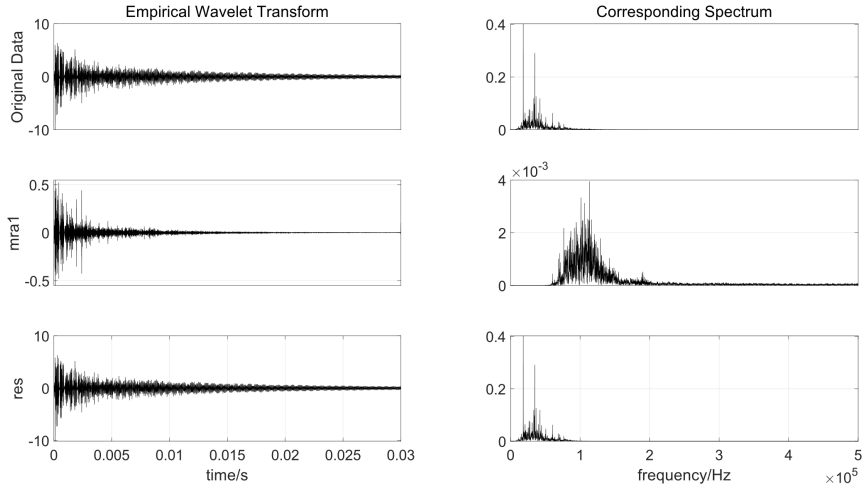


**Figure 6.** Modal decomposition of critical instability points for type 99 alumina ceramics.

**Table 1.** Characteristics of acoustic emission process of 95 zirconia ceramics.

| Damaged stage | Maximum energy/(mV*us) | Maximum amplitude/dB | AE count (energy >200mV*us)/times |
|---|---|---|---|
| 0 - 50 s | 359.9449 | 75.8 | 5 |
| 50 - 450 s | 646759.5734 | 73 | 1058 |
| 450 - 496 s | 443430.2208 | 98.6 | 29 |

**Table 2.** Characteristics of acoustic emission process of 99 alumina ceramics.

| Damaged stage | Maximum energy/(mV*us) | Maximum amplitude/dB | AE count (energy > 200 mV*us)/times |
|---|---|---|---|
| 0 - 30 s | 426.5442 | 66.7 | 1 |
| 30 - 100 s | 587069.4778 | 65.3 | 233 |
| 100 - 110 s | 309527.7702 | 99.2 | 19 |

stage, the amplitude of the signal remained the same as that of the crack propagation stage, resulting in less acoustic emission energy. There are various reasons for this. When the 95 zirconia ceramic first comes into contact with the bending mold, the bending mold and the ceramic specimen are running in. During this period, the 95 zirconia specimen only bends slightly, and the cracks do not nucleate and expand on a large scale. This is because brittle materials only undergo small elastic deformation and do not undergo plastic deformation. And it can monitor a certain amplitude of acoustic emission signals. During the crack propagation stage, more small cracks are generated and the original cracks expand. The nucleation and propagation of these cracks generate a large amount of acoustic emission signals. In the critical instability stage, the generation of acoustic emission energy decreases because small cracks have expanded into larger cracks. According to the percolation theory of acoustic emission and previous research on brittle materials, the propagation of larger cracks in brittle materials during the critical in-stability stage will generate low-frequency acoustic emission signals. 95% zirconia ceramics also basically conform to this characteristic. The energy and amplitude performance of 99 alumina ceramics is similar to that of 95 zirconia ceramics, but it is worth noting that during the entire acoustic emission process of 99 alumina ceramics, the AE energy released is lower, and the proportion in the initial stage is also larger. This indicates that 95 zirconia ceramics have higher rigidity and brittleness, which is an important characteristic that distinguishes their two properties.

### 3.3. Characterization of Acoustic Emission Damage Process

The formation and propagation of cracks in brittle materials under stress damage can stimulate the waveform of acoustic emission signals. The fracture process of brittle materials can generally be divided into three stages: crack nucleation, crack propagation, and ultimately unstable fracture. Under external forces, ceramic materials will transform into an unstable high-energy state near the cracks that originally existed, which will promote the continuous expansion of cracks.

The process of material damage under stress can trigger a large number of acoustic emission signals, which are rich in information and contain a lot of noise signals. Most of the time, the acoustic emission signals of crack propagation are mixed with machine noise, instrument noise, collision noise, etc. In continuous acoustic emission activities, a joint analysis overview can better reflect the original characteristics of material damage and deformation processes. As shown in **Figure 7** and **Figure 8**, the load application and amplitude distribution of acoustic emission signals are shown in the figures, and almost the entire acoustic emission process is accompanied by the generation of acoustic emission signals. The threshold voltage for acoustic emission set in this experiment is 40dB. As long as it exceeds the threshold voltage, it will be recorded and recorded as an acoustic emission impact event. The point with the highest amplitude in the acoustic emission impact event is considered to be the acoustic

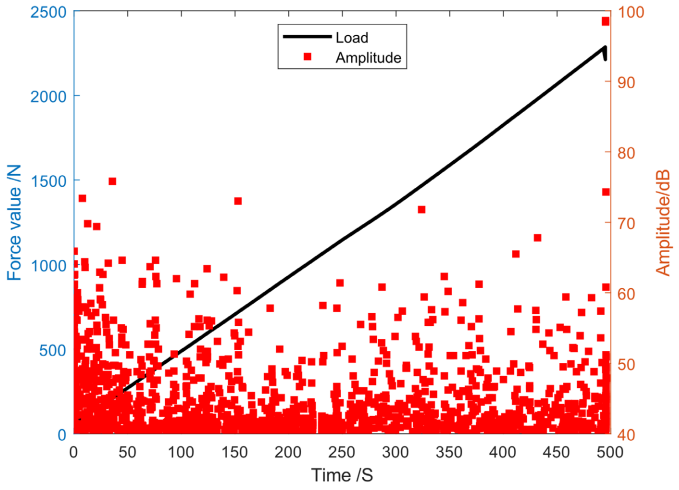


**Figure 7.** Load and signal amplitude diagram of type 95 zirconia ceramics.

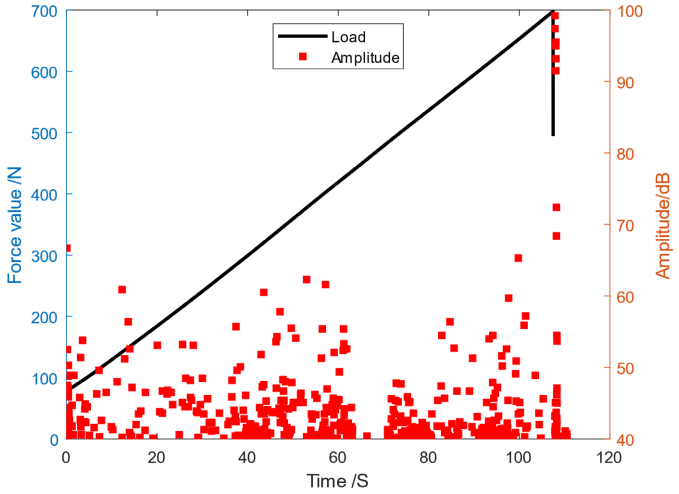


**Figure 8.** Load and signal amplitude diagram of type 99 alumina ceramics.

emission amplitude. From this, it can be concluded that there are many acoustic emission events during the initial compaction stage, which not only involve acoustic emission events generated by microcrack propagation, but also those generated by machine coupling and friction. Compared to 99 type alumina ceramics, 95 type zirconia ceramics exhibit more overall acoustic emission events, and the sudden disappearance of the load curve at the end of the acoustic emission process once again proves their high brittleness.

## 4. Empirical Conclusion

Through this experiment, we learned the differences in acoustic emission characteristics between 95 type zirconia ceramics and 99 type alumina ceramics during different stages of external force fracture. Overall, the fracture process of 95 type zirconia ceramics triggers much more acoustic emission signals than that

of 99 type alumina ceramics. At the same time, 95 type zirconia has higher bending strength and fracture instability. It can also be seen from the graph of loading force and acoustic emission amplitude that 95 type zirconia produces more acoustic emission events. However, the two types of ceramics also have many similarities, such as their deformation and damage processes, which excite higher acoustic emission amplitudes during the critical instability stage and can monitor a large amount of energy. They tend to emit acoustic emission signals with lower amplitudes during the crack propagation stage, and lower frequency acoustic emission signals are detected near the fracture stage, which can be considered as precursors to fracture. EWT decomposition + kurtosis + correlation coefficient analysis can more effectively evaluate the acoustic emission characteristics of two types of ceramics at the critical instability stage.

## Funding

The project is supported by Chongqing Natural Science Foundation (Project No. cstc2021jcyj msxmX0899).

## Conflicts of Interest

The authors declare no conflicts of interest regarding the publication of this paper.

## References

[1] El-Ghany, A.S.O. and Sherief, H.A. (2016) Zirconia Based Ceramics, Some Clinical and Biological Aspects: Review. *Future Dental Journal*, **2**, 55-64. https://doi.org/10.1016/j.fdj.2016.10.002

[2] Zhang, X., Wu, X. and Shi, J. (2020) Additive Manufacturing of Zirconia Ceramics: A State-of-the-Art Review. *Journal of Materials Research and Technology*, **9**, 9029-9048. https://doi.org/10.1016/j.jmrt.2020.05.131

[3] Zhu, Y., Liu, K., Deng, J., *et al.* (2019) 3D Printed Zirconia Ceramic Hip Joint with Precise Structure and Broad-Spectrum Antibacterial Properties. *International Journal of Nanomedicine*, **14**, 5977-5987. https://doi.org/10.2147/IJN.S202457

[4] Ivan, G., Elka, R. and Todor, U. (2021) Possibilities of Improving the Shear Strength between Different Type of Cement and Zirconia Ceramics: Literature Review. *Journal of IMAB*, **27**, 3557-3563. https://doi.org/10.5272/jimab.2021271.3557

[5] Gjurin, Z.S., Özcan, M. and Oblak, C. (2019) Zirconia Ceramic Fixed Partial Dentures after Cyclic Fatigue Tests and Clinical Evaluation: A Systematic Review. *Advances in Applied Ceramics*, **118**, 62-69. https://doi.org/10.1080/17436753.2018.1507428

[6] Dou, Y.X., Luo, S.H., Zhang, X., *et al.* (2023) Research Progress on Toughening Mechanism and Powder Preparation of Zirconia Ceramics. *Materials Introduction*, **37**, 134-139.

[7] Yan, J.Y., Guo, X.Y., Zhang, Y., *et al.* (2023) Research Progress on Doping Modification and Toughening Enhancement of Zirconia Based Structural Ceramics. *Contemporary Chemical Research*, **2**, 174-178.

[8] Xu, J., He, J., Xu, S., *et al.* (2018) Grinding Characteristics, Material Removal, and

Damage Formation Mechanisms of Zirconia Ceramics in Hybrid Laser/Grinding. *Journal of Manufacturing Science and Engineering*, **140**, Article ID: 071010. https://doi.org/10.1115/1.4039645

[9] Omar, B.F., Abhishek, S., Golam, K., *et al.* (2021) Parametric Study of Surface Characteristics of Laser Micro-Channel Milling of Zirconia ($ZrO_2$) at Defocused Condition. *Materials Today*: *Proceedings*, **47**, 2288-2292. https://doi.org/10.1016/j.matpr.2021.04.222

[10] Nasiry, L.K., Alma, R.S., Ali, T. and Zandinejad, A. (221) Additive Manufacturing of Zirconia Ceramic and Its Application in Clinical Dentistry: A Review. *Dentistry Journal*, **9**, Article 104. https://doi.org/10.3390/dj9090104

[11] Zhang, Z.L., Zhou, H.M., Feng, M., *et al.* (2023) Process Optimization of Magnetic Composite Fluid Polishing of Zirconia Ceramics. *Diamond and Absolute Engineering*, **43**, 712-719. http://www.jgszz.cn/article/doi/10.13394/j.cnki.jgszz.2023.0003

[12] Russo, S.D., Cinelli, F., Sarti, C. and Giachetti, L. (2019) Adhesion to Zirconia: A Systematic Review of Current Conditioning Methods and Bonding Materials. *Dentistry Journal*, **7**, Article 74. https://doi.org/10.3390/dj7030074

[13] Farhad, T. (2019) Color Aspect of Monolithic Zirconia Restorations: A Review of the Literature. *Journal of Prosthodontics*, **28**, 276-287. https://doi.org/10.1111/jopr.12906

[14] Shahmiri, R., Standard, C.O., Hart, N.J. and Sorrell, C.C. (2018) Optical Properties of Zirconia Ceramics for Esthetic Dental Restorations: A Systematic Review. *The Journal of Prosthetic Dentistry*, **119**, 36-46. https://doi.org/10.1016/j.prosdent.2017.07.009

[15] Al-Aali, A.K. (2018) Effect of Phototherapy on Shear Bond Strength of Resin Cements to Zirconia Ceramics: A Systematic Review and Meta-Analysis of *in-Vitro* Studies. *Photodiagnosis and Photodynamic Therapy*, **23**, 58-62. https://doi.org/10.1016/j.pdpdt.2018.05.006

[16] Zhuo, R., Deng, Z., Chen, B., *et al.* (2021) Overview on Development of Acoustic Emission Monitoring Technology in Sawing. *The International Journal of Advanced Manufacturing Technology*, **116**, 1411-1427. https://doi.org/10.1007/s00170-021-07559-5

[17] He, Y., Li, M., Meng, Z., *et al.* (2021) An Overview of Acoustic Emission Inspection and Monitoring Technology in the Key Components of Renewable Energy Systems. *Mechanical Systems and Signal Processing*, **148**, Article ID: 107146. https://doi.org/10.1016/j.ymssp.2020.107146

[18] Guo, L., Huo, K.L. and Guo, J.T. (2019) Acoustic Emission Monitoring of Diamond Grinding Wheel Wear Status Based on EMD. *Journal of Hunan University* (*Natural Science Edition*), **46**, 58-66.

[19] Gass, E.S., Sandoval, L.M., Talou, H.M., *et al.* (2015) High Temperature Mechanical Behavior of Porous Cordierite-Based Ceramic Materials Evaluated Using 3-Point Bending. *Procedia Materials Science*, **9**, 254-261. https://doi.org/10.1016/j.mspro.2015.04.032

[20] Sundh, A. and Sjögren, G. (2007) A Study of the Bending Resistance of Implant-Supported Reinforced Alumina and Machined Zirconia Abutments and Copies. *Dental Materials*, **24**, 611-617. https://doi.org/10.1016/j.dental.2007.05.021

[21] Giridhar, D., Vijayaraghavan, L. and Krishnamurthy, R. (2011) Acoustic Emission Response of Sintered Alumina Zirconia Composite during Grooving Process. *NDT and E International*, **46**, 55-62. https://doi.org/10.1016/j.ndteint.2011.11.002

[22] Chu, L. (2015) Research on Acoustic Emission Characteristics of Ceramic Material Failure Process and Toughening Effect. Master's Thesis, Beijing Institute of Technology, Beijing.

[23] Chang, Z.S. (2016) Research on Toughened Ceramic Damage Based on Acoustic Emission Technology. Master's Thesis, Beijing Institute of Technology, Beijing.

[24] Lan, Y.X., Liu, W., Li, N., *et al.* (2023) The Effect of Bubble Defects on the Fracture Toughness of Zirconia Ceramics. *Journal of Composite Materials*, **40**, 6809-6818.

[25] Yuan, Z.Q., Li, Z.F., Chen, J.X., *et al.* (2023) $CaO/Y_2O_3$ Co Stable ZrO Study on the Microstructure and Mechanical Properties of 2-Phase Ceramics. *Chinese Ceramics*, **59**, 22-29.

[26] Rodaev, V.V., *et al.* (2021) An Engineering Zirconia Ceramic Made of Baddeleyite. *Materials*, **14**, Article 4676. https://doi.org/10.3390/ma14164676

[27] Rukiye, D., Gonca, G.D., Hatice, Ş., *et al.* (2021) Biaxial Flexural Strength and Phase Transformation Characteristics of Dental Monolithic Zirconia Ceramics with Different Sintering Durations: An *in Vitro* Study. *The Journal of Prosthetic Dentistry*, **128**, 498-504. https://doi.org/10.1016/j.prosdent.2021.04.003

[28] Zhao, K., Yang, X., Xiong, L.F., *et al.* (2023) Damage Characteristics of Stable Crack Propagation Stage in Sandstone with Different Water Content States. Metal Mines. https://kns-cnki-net.webvpn.las.ac.cn/kcms/detail/34.1055.TD.20230522.1826.002.html

[29] Sun, Z.Q., Xie, L.Z., Liu, J.F., *et al.* (2014) Research on Damage and Failure of Salt Rock Based on Percolation Model. *Geotechnical Mechanics*, **35**, 441-448.

[30] Tang, X.J., Tian, X.L., Wang, L., *et al.* (2016) Acoustic Emission Percolation Characteristics of Engineering Ceramic Fragmentation Damage. *Acta Acoustica Sinica*, **41**, 195-201.

[31] Sakhaee-Pour, A. and Agrawal, A. (2018) Integrating Acoustic Emission into Percolation Theory to Predict Permeability Enhancement. *Journal of Petroleum Science and Engineering*, **160**, 152-159. https://doi.org/10.1016/j.petrol.2017.10.003

[32] Gilles, J. (2013) Empirical Wavelet Transform. *IEEE Transactions on Signal Processing*, **61**, 3999-4010. https://doi.org/10.1109/TSP.2013.2265222